

## Separating Exchange Splitting from Spin Mixing in Gadolinium by Femtosecond Laser Excitation

Beatrice Andres,<sup>\*</sup> Marc Christ, Cornelius Gahl, Marko Wietstruk, and Martin Weinelt  
*Freie Universität Berlin, Fachbereich Physik, Arnimallee 14, 14195 Berlin, Germany*

Jürgen Kirschner

*Max-Planck-Institut für Mikrostrukturphysik, Weinberg 2, 06120 Halle/Saale, Germany*

(Received 2 July 2015; published 10 November 2015)

Employing spin-, time-, and energy-resolved photoemission spectroscopy, we present the first study on the spin polarization of a single electronic state after ultrafast optical excitation. Our investigation concentrates on the majority-spin component of the  $d$ -band-derived Gd(0001) surface state  $d_{z^2}^{\uparrow}$ . While its binding energy shows a rapid Stoner-like shift by 90 meV with an exponential time constant of  $\tau_E = 0.6 \pm 0.1$  ps, the  $d_{z^2}^{\uparrow}$  spin polarization remains nearly constant within the first picoseconds and decays with  $\tau_S = 15 \pm 8$  ps. This behavior is in clear contrast to the equilibrium phase transition, where the spin polarization vanishes at the Curie temperature.

DOI: 10.1103/PhysRevLett.115.207404

PACS numbers: 78.47.-p, 71.45.Gm, 73.20.At

Laser excitation is capable of creating new transient states of matter, that are not reached on equilibrium pathways [1–6]. In magnetically ordered materials this opens new routes to the ultrafast manipulation of the magnetic order [7–10]. Investigating the underlying processes provides a yet unseen view on the very basics of magnetism such as the relation between the electronic and magnetic structure. Contrary to thermal heating, laser excitation drives the electronic, phonon, and spin subsystems out of equilibrium [11]. It may therefore lead to a response quite different from the equilibrium magnetic phase transition as we show in this Letter.

The first experiment on the laser-induced demagnetization of Gd metal applied spin-resolved photoemission on the nanosecond time scale [12]. A decrease of the spin polarization of the secondary electrons was observed, which was explained by spin-lattice relaxation with a characteristic time of  $100 \pm 80$  ps. This result was corroborated by measurements of the magnetic linear dichroism (MLD) observed in  $4f$  core-level photoemission [13]. Later studies with sub-ps time resolution revealed an additional much faster decrease of magnetic figures: The x-ray magnetic circular dichroism (XMCD) at the  $M_5$  edge decreases within  $0.76 \pm 0.25$  ps [14]. So do rotation and ellipticity of the magneto-optical Kerr effect (MOKE) [15,16] as well as the ( $5d6s$ ) valence-band exchange splitting [17,18]. A binding energy shift on this time scale has also been found for the majority-spin component of the surface state [19,20]. In contrast, the magnetic component of the surface-sensitive second harmonic generation (SHG) shows an immediate response within the laser pulse duration of 100 fs [19,21,22]. Whereas a recent photoemission experiment reveals again a ps response of the MLD in the  $4f$  states [23]. Obviously, different observables

of the magnetization dynamics suggest significantly different response times, while in the equilibrium phase transition all techniques map the same behavior. Furthermore, most of the femtosecond pump-probe experiments are not consistent with the spin-resolved measurements of Ref. [12], which may be attributed to its 10-ns pump-pulse duration. It is thus still unclear on which time scale we can modify the spin polarization in Gd using an ultrafast laser pulse.

In this Letter we present a comparative study of equilibrium vs laser-induced demagnetization of Gd using spin-resolved photoemission. Upon excitation with a 48-fs laser pulse the majority-spin component  $d_{z^2}^{\uparrow}$  of the Gd surface state shifts towards the Fermi level, reducing the exchange splitting on a sub-ps time scale. In contrast, the  $d_{z^2}^{\uparrow}$  spin polarization changes only slightly with a 1 order of magnitude slower ps dynamics.

For the pump we use  $s$ -polarized pulses at the fundamental photon energy of 1.6 eV of a 300-kHz Ti:sapphire regenerative amplifier (RegA, Coherent) incident at an angle of  $45^\circ$  off normal along the Gd[1000] direction. The absorbed pump fluence was  $3.9$  mJ/cm<sup>2</sup>. A time-delayed  $p$ -polarized ultraviolet probe is generated by frequency quadrupling the fundamental to 6.3 eV. The temporal resolution is  $\leq 70$  fs as determined from fitting the rising edge of the electronic temperature [Fig. 3(a)]. A cylindrical sector analyzer (CSA 300, Focus) transmits the photoemitted electrons to the spin detector with an energy and angular resolution of 65 meV and  $\pm 2.5^\circ$ , respectively. We use an exchange-scattering-based spin detector [24], which supports two measurement modes: A spin-integrated mode, where all incoming electrons impinge directly on a channeltron, and a spin-resolved mode, where we place an oxygen-passivated Fe/W(001) target into the electron

beam for spin-dependent exchange scattering at 6 eV kinetic energy into a second channeltron in back-reflection geometry. The spin detector has a figure of merit of  $2.2 \times 10^{-3}$  with an intensity loss of 2 orders of magnitude [24]. We took advantage of switching on the fly between the spin-integrated and spin-resolved mode, to acquire high-intensity spin-integrated data on the energetic behavior and valuable information on the spin polarization in the same experiment. The investigated Gd(0001) samples were prepared by evaporating 100 Å of Gd onto a W(110) substrate at a temperature of 300 K, a deposition rate of 5 Å/min and a pressure of  $6 \times 10^{-10}$  mbar. Beforehand, the substrate was cleaned from carbon impurities as described in Ref. [25]. To obtain a smooth and contaminant-free surface, the Gd films were annealed for 1 min at 780 K. During the measurements at a pressure of  $2 \times 10^{-11}$  mbar, we kept a sample temperature of 90 K by liquid nitrogen cooling. All spectra were taken at  $\bar{\Gamma}$  under normal emission. The Gd films were magnetized to remanence in plane along the Gd[1100] direction applying a field pulse of 20 mT via a freestanding coil.

The ferro- to paramagnetic phase transition of gadolinium at the Curie temperature  $T_C = 293$  K is a prototype system to study spin mixing vs Stoner behavior. The latter two limiting cases turned out to be helpful for distinguishing the temperature dependence of the electronic structure of a ferromagnet in thermal equilibrium. The Stoner model [26–29] treats delocalized electronic states and predicts a gradual decrease of the exchange splitting, which collapses at  $T_C$ . By contrast, spin mixing [30–34] describes localized states with a constant magnitude but fluctuating direction of the magnetic moment. In this model the exchange splitting stays constant while the spin polarization of the states falls steadily with increasing temperature to vanish at  $T_C$ .

Evidence for the existence of a finite exchange splitting above  $T_C$  has been found in the Gd(0001) surface state [35–39], where the majority- (minority-) spin component  $d_{z_2}^{\uparrow}$  ( $d_{z_2}^{\downarrow}$ ) is situated below (above) the Fermi level  $E_F$ . Figure 1 displays the temperature-dependent spin polarization (a) and binding energy  $E - E_F$  (b) of the  $d_{z_2}^{\uparrow}$  determined by spin-resolved laser photoemission with 4.5 eV photons. When Gd(0001) is heated across  $T_C$  the  $d_{z_2}^{\uparrow}$  spin polarization collapses while its exchange splitting is only partly lowered but remains at finite values. For more than 100 K above  $T_C$ , the  $d_{z_2}^{\uparrow}$  remains below  $E_F$  [38] while the minority-spin part still has a binding energy above  $E_F$  [35–37]. To conclude, in the equilibrium phase transition the surface state shows spin mixing accompanied by a partly decreasing exchange splitting, i.e., a partly Stoner-like behavior.

In the following, we investigate the laser-driven phase transition. The spin-integrated photoemission intensity near  $E_F$  is shown in Fig. 2(a) as a function of energy  $E - E_F$  and pump-probe delay. Figure 2(b) compares the majority- and

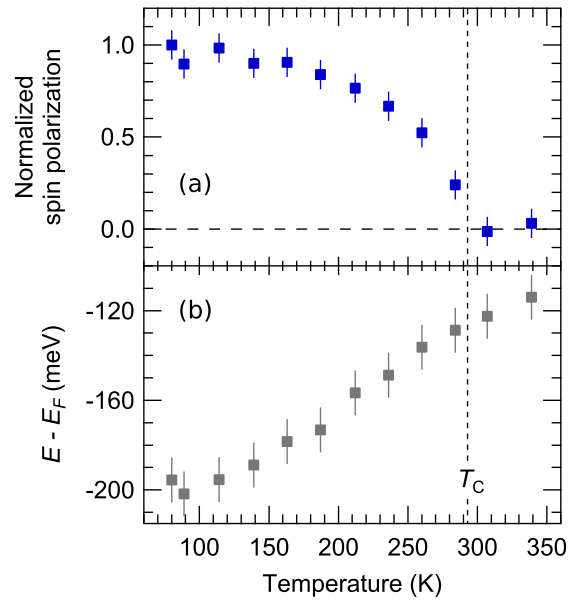


FIG. 1 (color online). Spin polarization (a) and binding energy (b) of the majority-spin surface state  $d_{z_2}^{\uparrow}$  in the ferro- to paramagnetic phase transition in thermal equilibrium. The spin polarization vanishes at  $T_C = 293$  K but the exchange splitting remains finite.

minority-spin intensities at selected delays. Independent of spin, there is a remarkable intensity redistribution after the excitation by the pump pulse at 0 ps. Compared to the spectra before pumping at  $-0.5$  ps, the  $d_{z_2}^{\uparrow}$  surface state is significantly depopulated at 0.2 ps and electrons are excited above  $E_F$ . This redistribution is attributed to an increasing electronic temperature reflected in a broadening of the Fermi edge as well as a broadening of the surface-state line shape. In addition, the maximum of the  $d_{z_2}^{\uparrow}$  shifts to lower binding energy [indicated by the gray horizontal bars in Fig. 2(b)]. Directly after laser excitation, at a delay of 0.2 ps, the peak position is shifted by 27 meV towards  $E_F$ . This shift increases to 90 meV at 10 ps delay, when the population of the  $d_{z_2}^{\uparrow}$  already recovers, most of the laser-excited electron population above  $E_F$  is decayed, and electron and phonon subsystems are equilibrated at an elevated temperature [40]. At this temperature a part of the peak is cut by the broad Fermi edge, such that the peak position obtained from a fit to the data (indicated by the gray bar) is closer to  $E_F$  as the maximum intensity visible in the spectrum [41]. Sample cooling shifts the  $d_{z_2}^{\uparrow}$  binding energy back to the initial value and the broadening of line shape and Fermi edge further reduces as exemplified by the spectrum at 50 ps delay. Despite these significant changes, the ratio of majority- and minority-spin intensity and thus the spin polarization alters only weakly for all displayed pump-probe delays.

For a more detailed discussion, the temporal evolutions of the above-mentioned parameters: electronic temperature,

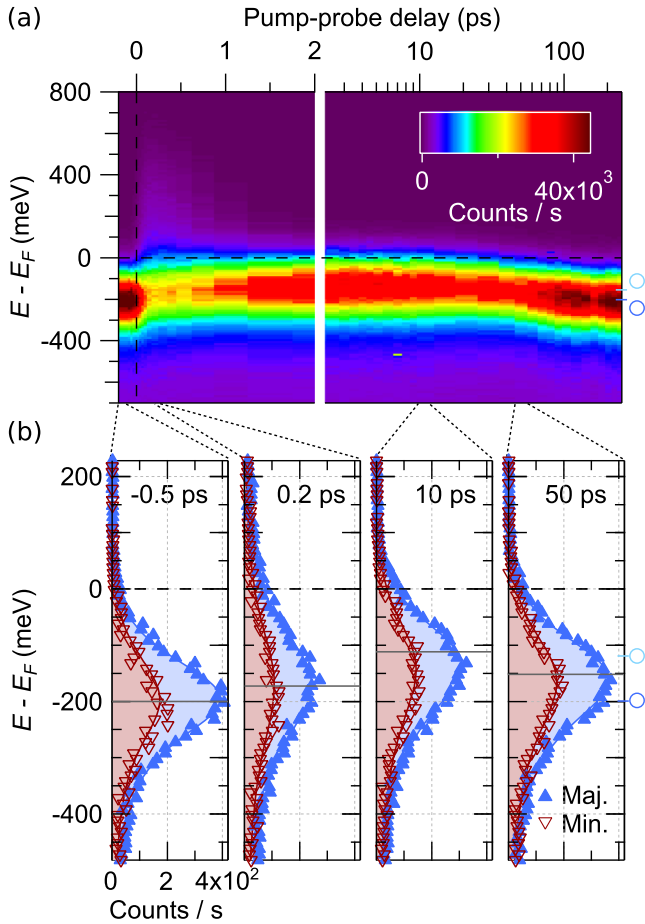


FIG. 2 (color online). (a) False color representation of spin-integrated photoemission spectra of the gadolinium  $d_{z^2}^{\uparrow}$  surface state as a function of pump-probe delay. (b) Spin-resolved photoemission spectra at selected pump-probe delays. The spin polarization [asymmetry between majority (closed triangle) and minority (inverted triangle) count rates] shows only weak changes in all four spectra.

surface-state binding energy, and spin polarization are shown in Fig. 3. The data were obtained from a fit to the spectra as described in the Supplemental Material [41]. The spin polarization calculates as  $P = [(I^{\uparrow} - I^{\downarrow}) / (I^{\uparrow} + I^{\downarrow})]$ , where  $I^{\uparrow(\downarrow)}$  is either the intensity integrated over the energy range of the full majority(minority) peak ( $\bullet$ ) or the photoemission intensity measured at a single binding energy ( $\circ$ ). Integrating over the full peak yields more accurate values but also requires a lot more data acquisition time and is thus more susceptible to changes of the surface quality. We therefore complemented the data by measurements at distinct energies with a significant spin polarization. Here we chose the maximal and minimal binding energy of the  $d_{z^2}^{\uparrow}$  of  $-200$  and  $-120$  meV ( $\circ$ ) (indicated in Fig. 2 on the right ordinate) [42].

Figure 3(a) shows the immediate increase of the electronic temperature up to 2000 K within the temporal resolution of 70 fs. The subsequent temporal evolution

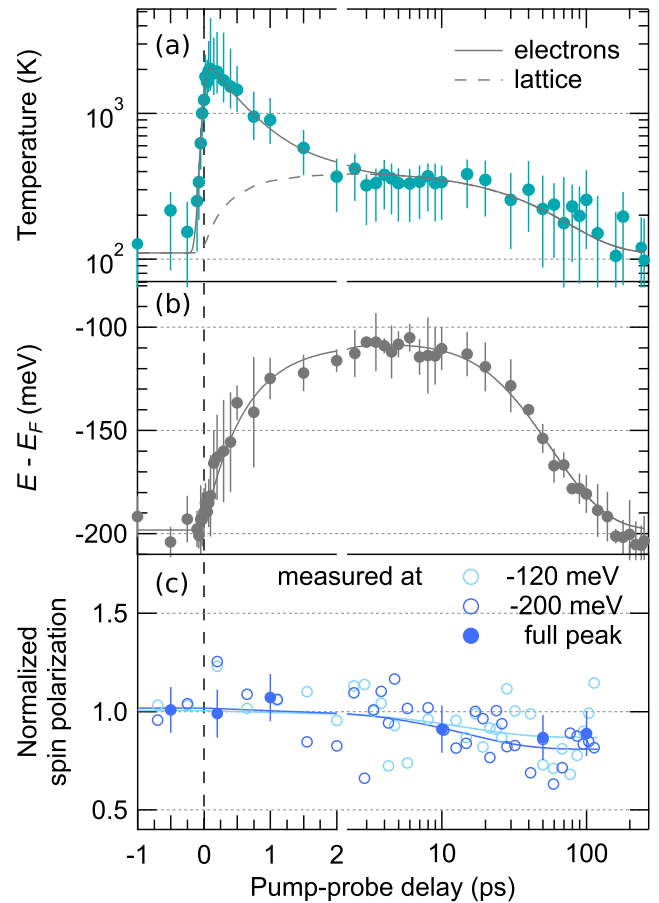


FIG. 3 (color online). Temporal evolution of (a) electronic temperature as obtained from the broadening of the Fermi edge, (b) binding energy, and (c) spin polarization of the  $d_{z^2}^{\uparrow}$ . The spin polarization integrated over the energy range of the full peak (circle) is complemented by data taken at 120 and 200 meV (open circle) binding energy indicated in Fig. 2 on the right ordinate.

of the temperature within the first picoseconds can be described (solid line) by an exponential decay that is overlaid by a rise in lattice temperature (dashed line). We thus assume that the electrons cool down predominantly transferring energy to the lattice at a time constant of  $\tau_E = 0.6 \pm 0.1$  ps. We find that the shift in binding energy [Fig. 3(b)] occurs with the same exponential time constant  $\tau_E$  and must therefore be induced by a heating of the lattice due to electron-phonon scattering. Thus, the peak position is determined by the lattice temperature. This is in perfect agreement with the results in the equilibrium phase transition (cf. Fig. 1). In contrast, the spin polarization itself shows in fact a much slower decrease of small magnitude. An exponential fit to the spin polarization results in a decay time of  $\tau_S = 15 \pm 8$  ps (dark and light blue lines for  $-200$  and  $-120$  meV). This slow decrease can already be explained by spin-lattice coupling as has been suggested in Ref. [12].

The evolutions of the spin polarization in the laser-driven experiment and in the thermal phase transition (filament

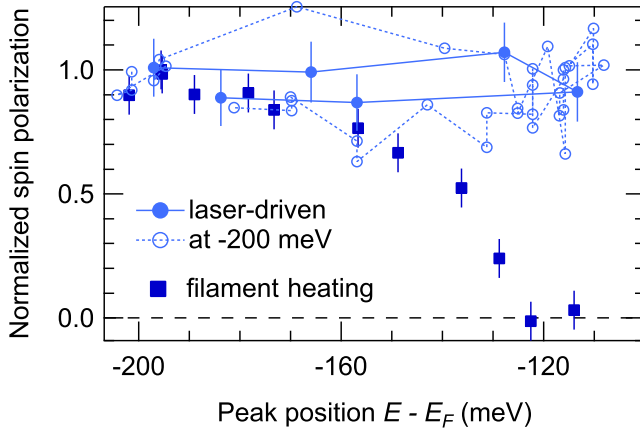


FIG. 4 (color online). Comparison of laser-driven (circles) and thermal phase transition (squares). The spin polarization is plotted vs the binding energy corresponding to a pump-probe delay or temperature, respectively. Open circles display the spin polarization obtained at a single energy ( $-200$  meV). Closed circles show energy-integrated values for the full  $d_{z_2}^\uparrow$  peak. The uncertainties of the peak position are shown in Figs. 1 and 3.

heating) are compared in Fig. 4. The bottom axis shows the corresponding peak energy for each temperature in the equilibrium experiment ( $\blacksquare$ ) and for each pump-probe delay in the laser-driven experiment ( $\bullet$ ,  $\circ$ ), respectively. We find that upon optical excitation the peak position shifts to  $E - E_F = -110$  meV with almost no decrease in spin polarization. In the equilibrium phase transition, the  $d_{z_2}^\uparrow$  already loses its spin polarization when it reaches the same energy, since this is when the sample is heated across  $T_C$  (cf. Fig. 1). In the laser-driven experiment we observe a small reduction of the spin polarization to  $\sim 0.9$ , which is much slower than the changes in binding energy. The reduced spin polarization remains during the cooling of the lattice when the peak energy is already shifting back.

It has been reported for a photoemission experiment with a lower pump fluence of  $1 \text{ mJ/cm}^2$  [19] that the  $d_{z_2}^\uparrow$  shift has not much effect on the total exchange splitting of the surface state. Nevertheless, experiments applying fluences similar to that in our experiment, find a breakdown of magnetic signals like XMCD [14] or MOKE [15] occurring on the same time scale as the  $d_{z_2}^\uparrow$  shift. Also the exchange splitting of the ( $5d6s$ ) valence bands decreases with the same time constant [17,18]. Therefore, we interpret the shift in our experiment as a change in exchange splitting, which is not accompanied by a reduction of spin polarization. We thus demonstrate that the response of the Gd(0001)  $d_{z_2}^\uparrow$  surface state to an ultrafast laser excitation is completely Stoner-like within the first picoseconds. While in the equilibrium phase transition Stoner and spin-mixing behavior occur simultaneously, in the laser-driven experiment the spin

polarization decreases exponentially with  $\tau_S = 15 \pm 8$  ps subsequent to the Stoner-like change of the binding energy with  $\tau_E = 0.6 \pm 0.1$  ps.

Three processes are reflected in the dynamics of the  $d_{z_2}^\uparrow$  surface state. (i) The fastest process, the direct heating of the electrons by the laser ( $< 70$  fs), causes the fast response found in magnetic SHG [19,21,22]. According to Ref. [21], the highly spin-polarized surface state contributes dominantly to the SHG process. Thus, its depopulation lowers the magnetic component of the signal. (ii) Subsequently, energy is transferred from the electrons to the lattice, thereby inducing the Stoner-like shift of  $d_{z_2}^\uparrow$  with  $\tau_E = 0.6 \pm 0.1$  ps. MOKE depends on all possible transitions in the Brillouin zone [43]. It is therefore sensitive to the exchange splitting of the ( $5d6s$ ) bands and, hence, shows a corresponding response time. It is, however, surprising that the XMCD contrast at the  $M_5$  edge decreases on this time scale as well [14]. (iii) XMCD and MOKE also reveal a second time scale in the 10 ps regime similar to the response we find in the  $d_{z_2}^\uparrow$  spin polarization. Recent results revealed that the MLD in photoemission from the  $4f$  core levels decreases on the same slow ps time scale [23]. This suggests that the spin polarization of the valence states is determined by the  $4f$  magnetic moment [44]. Such a demagnetization on two distinct time scales was already predicted by Koopmans *et al.* [45], but their model is solely based on a mean field description. It does not distinguish between exchange splitting and spin polarization, and, hence, misses important ingredients to describe the magnetization dynamics of  $4f$  metals.

It is reasonable to assume that the observed behavior is characteristic for Gd, since spin-resolved photoemission measurements on Fe and Ni find an ultrafast breakdown of the overall spin polarization, though without orbital resolution [43,46,47].

In conclusion, we find that the response times of spin polarization and exchange splitting differ by more than 1 order of magnitude. This leads to a Stoner-like behavior of the surface state during the first picoseconds. We expect the huge difference between the Stoner and spin-mixing time scales in Gd to arise from the indirect exchange interaction. While the ( $5d6s$ ) valence electrons are directly affected by the laser excitation leading to the decreasing exchange splitting, the  $4f$  spin system remains cold for a long time, stabilizing the spin polarization [23]. In contrast, in the equilibrium phase transition, these processes cannot be separated. Using ultrafast laser excitation, we are able to disentangle exchange splitting and spin polarization, which opens a completely new view on the magnetic phase transition.

We thank the Helmholtz Virtual Institute ‘‘Dynamic Pathways in Multidimensional Landscapes’’ and the DFG for financial support.

- \*Corresponding author.  
andres@physik.fu-berlin.de
- [1] A. Cavalleri, C. Tóth, C. W. Siders, J. A. Squier, F. Rákai, P. Forget, and J. C. Kieffer, *Phys. Rev. Lett.* **87**, 237401 (2001).
- [2] L. Perfetti, P. A. Loukakos, M. Lisowski, U. Bovensiepen, H. Berger, S. Biermann, P. S. Cornaglia, A. Georges, and M. Wolf, *Phys. Rev. Lett.* **97**, 067402 (2006).
- [3] D. Fausti, R. I. Tobey, N. Dean, S. Kaiser, A. Dienst, M. C. Hoffmann, S. Pyon, T. Takayama, H. Takagi, and A. Cavalleri, *Science* **331**, 189 (2011).
- [4] L. Stojchevska, I. Vaskivskiy, T. Mertelj, P. Kusar, D. Svetin, S. Brazovskii, and D. Mihailovic, *Science* **344**, 177 (2014).
- [5] D. Wegkamp, M. Herzog, L. Xian, M. Gatti, P. Cudazzo, C. L. McGahan, R. E. Marvel, R. F. Haglund, A. Rubio, M. Wolf, and J. Stähler, *Phys. Rev. Lett.* **113**, 216401 (2014).
- [6] M. Dell'Angela *et al.*, *Science* **339**, 1302 (2013).
- [7] I. Radu, K. Vahaplar, C. Stamm, T. Kachel, N. Pontius, H. A. Dürr, T. A. Ostler, J. Barker, R. F. L. Evans, R. W. Chantrell, A. Tsukamoto, A. Itoh, A. Kirilyuk, T. Rasing, and A. V. Kimel, *Nature (London)* **472**, 205 (2011).
- [8] C. D. Stanciu, F. Hansteen, A. V. Kimel, A. Kirilyuk, A. Tsukamoto, A. Itoh, and T. Rasing, *Phys. Rev. Lett.* **99**, 047601 (2007).
- [9] A. Kirilyuk, A. V. Kimel, and T. Rasing, *Rev. Mod. Phys.* **82**, 2731 (2010).
- [10] S. Mangin, M. Gottwald, C.-H. Lambert, D. Steil, V. Uhlir, L. Pang, M. Hehn, S. Alebrand, M. Cinchetti, G. Malinowski, Y. Fainman, M. Aeschlimann, and E. E. Fullerton, *Nat. Mater.* **13**, 286 (2014).
- [11] E. Beaupaire, J.-C. Merle, A. Daunois, and J.-Y. Bigot, *Phys. Rev. Lett.* **76**, 4250 (1996).
- [12] A. Vaterlaus, T. Beutler, and F. Meier, *Phys. Rev. Lett.* **67**, 3314 (1991).
- [13] A. Melnikov, H. Prima-Garcia, M. Lisowski, T. Giessel, R. Weber, R. Schmidt, C. Gahl, N. M. Bulgakova, U. Bovensiepen, and M. Weinelt, *Phys. Rev. Lett.* **100**, 107202 (2008).
- [14] M. Wietstruk, A. Melnikov, C. Stamm, T. Kachel, N. Pontius, M. Sultan, C. Gahl, M. Weinelt, H. A. Dürr, and U. Bovensiepen, *Phys. Rev. Lett.* **106**, 127401 (2011).
- [15] M. Sultan, U. Atxitia, A. Melnikov, O. Chubykalo-Fesenko, and U. Bovensiepen, *Phys. Rev. B* **85**, 184407 (2012).
- [16] M. Sultan, A. Melnikov, and U. Bovensiepen, *Phys. Status Solidi B* **248**, 2323 (2011).
- [17] R. Carley, K. Döbrich, B. Frietsch, C. Gahl, M. Teichmann, O. Schwarzkopf, P. Wernet, and M. Weinelt, *Phys. Rev. Lett.* **109**, 057401 (2012).
- [18] M. Teichmann, B. Frietsch, K. Döbrich, R. Carley, and M. Weinelt, *Phys. Rev. B* **91**, 014425 (2015).
- [19] M. Lisowski, P. A. Loukakos, A. Melnikov, I. Radu, L. Ungureanu, M. Wolf, and U. Bovensiepen, *Phys. Rev. Lett.* **95**, 137402 (2005).
- [20] P. A. Loukakos, M. Lisowski, G. Bihlmayer, S. Blügel, M. Wolf, and U. Bovensiepen, *Phys. Rev. Lett.* **98**, 097401 (2007).
- [21] A. Melnikov, I. Radu, U. Bovensiepen, O. Krupin, K. Starke, E. Matthias, and M. Wolf, *Phys. Rev. Lett.* **91**, 227403 (2003).
- [22] A. Melnikov, I. Radu, A. Povolotskiy, T. Wehling, A. Lichtenstein, and U. Bovensiepen, *J. Phys. D* **41**, 164004 (2008).
- [23] B. Frietsch, J. Bowlan, R. Carley, M. Teichmann, S. Wienholdt, D. Hinzke, U. Nowak, K. Carva, P. M. Oppeneer, and M. Weinelt, *Nat. Commun.* **6**, 8262 (2015).
- [24] A. Winkelmann, D. Hartung, H. Engelhard, C.-T. Chiang, and J. Kirschner, *Rev. Sci. Instrum.* **79**, 083303 (2008).
- [25] B. Andres, P. Weiss, M. Wietstruk, and M. Weinelt, *J. Phys. Condens. Matter* **27**, 015503 (2015).
- [26] E. C. Stoner, *Proc. R. Soc. A* **154**, 656 (1936).
- [27] J. C. Slater, *Phys. Rev.* **49**, 537 (1936).
- [28] J. C. Slater, *Phys. Rev.* **49**, 931 (1936).
- [29] E. C. Stoner, *Proc. R. Soc. A* **165**, 372 (1938).
- [30] V. Korenman, J. L. Murray, and R. E. Prange, *Phys. Rev. B* **16**, 4032 (1977).
- [31] H. Capellmann, *Z. Phys. B* **34**, 29 (1979).
- [32] H. Hasegawa, *J. Phys. Soc. Jpn.* **46**, 1504 (1979).
- [33] R. E. Prange and V. Korenman, *Phys. Rev. B* **19**, 4691 (1979).
- [34] A. J. Pindor, J. Staunton, G. M. Stocks, and H. Winter, *J. Phys. F* **13**, 979 (1983).
- [35] M. Bode, M. Getzlaff, S. Heinze, R. Pascal, and R. Wiesendanger, *Appl. Phys. A* **66**, S121 (1998).
- [36] M. Getzlaff, M. Bode, S. Heinze, R. Pascal, and R. Wiesendanger, *J. Magn. Magn. Mater.* **184**, 155 (1998).
- [37] M. Donath, B. Gubanka, and F. Passek, *Phys. Rev. Lett.* **77**, 5138 (1996).
- [38] E. Weschke, C. Schüssler-Langeheine, R. Meier, A. V. Fedorov, K. Starke, F. Hübinger, and G. Kaindl, *Phys. Rev. Lett.* **77**, 3415 (1996).
- [39] K. Maiti, M. C. Malagoli, A. Dallmeyer, and C. Carbone, *Phys. Rev. Lett.* **88**, 167205 (2002).
- [40] U. Bovensiepen, *J. Phys. Condens. Matter* **19**, 083201 (2007).
- [41] See Supplemental Material at <http://link.aps.org/supplemental/10.1103/PhysRevLett.115.207404> for a decomposition of the fit.
- [42] See Supplemental Material at <http://link.aps.org/supplemental/10.1103/PhysRevLett.115.207404> for the corresponding spin-resolved photoemission intensities.
- [43] A. Weber, F. Pressacco, S. Günther, E. Mancini, P. M. Oppeneer, and C. H. Back, *Phys. Rev. B* **84**, 132412 (2011).
- [44] L. M. Sandratskii, *Phys. Rev. B* **90**, 184406 (2014).
- [45] B. Koopmans, G. Malinowski, F. Dalla Longa, D. Steiauf, M. Fahnle, T. Roth, M. Cinchetti, and M. Aeschlimann, *Nat. Mater.* **9**, 259 (2010).
- [46] A. Fognini *et al.*, *Appl. Phys. Lett.* **104**, 032402 (2014).
- [47] A. Scholl, L. Baumgarten, R. Jacquemin, and W. Eberhardt, *Phys. Rev. Lett.* **79**, 5146 (1997).